Monte Carlo simulations for the analysis of texture and strain measured with Bragg edge neutron transmission

Monte Carlo simulations for the analysis of texture and strain measured with Bragg edge neutron transmission

M Boin[1,2], R C Wimpory[1], A Hilger[1], N Kardjilov[1], S Y Zhang[3] and M Strobl[1]

[1]Helmholtz Centre Berlin for Materials and Energy, Hahn-Meitner-Platz 1, 14109 Berlin, Germany
[2]The Open University, Walton Hall, Milton Keynes, MK7 6AA, England
[3]ISIS Facility, Rutherford Appleton Laboratory, Chilton, Didcot, OX11 OQX, England

boin@helmholtz-berlin.de

Abstract. The transmission spectrum of cold and thermal neutrons displays sudden intensity changes, known as Bragg edges, whose appearance is connected to the crystallographic structure of the investigated sample. However, many difficulties in interpreting and understanding the detected signal exist, in particular when results are evaluated quantitatively. We measured strain and texture properties of different samples utilizing the Bragg edge method on the CONRAD and VSANS instruments at Helmholtz Centre Berlin as well as on ENGIN-X at ISIS, UK. The different results will be compared and validated with conventional diffraction measurements and theoretical considerations. According to this, a Bragg edge neutron transmission simulation was developed to include instrument effects together with sample characteristics. Therefore, a neutron ray-tracing simulation package was applied to emulate the employed instruments in combination with the Bragg edge transmission technique. A new sample module has been created to realize energy-dependent transmission simulations based on neutron cross sections calculations. Towards the analysis of the conducted experiments the virtual sample features the expected strain and texture parameters. The results of the simulation are in good agreement with the experiments and will be discussed with regard to the prospects and limitations of this measurement method and the utilized instruments.

1. Introduction

Monte Carlo simulations have become more and more an important tool for the development of neutron instruments and experimental data analysis [1, 2]. Due to the complexity of a neutron instrument, a large number of parameters must be considered when instrument optimizations and new beamlines are realized. The valuation of the instrument's influences on the measured detector signal is useful when more flux or higher resolution, for example, are aimed at and extra effects to the detector signal must be quantified. A Monte Carlo neutron instrument simulation therefore enables the testing of varying parameters while their influences on the sample position and the detector are monitored. Furthermore, a simulation could be utilized to study the feasibility of alternative measurement methods. Then, the value of the measured results could be validated by a comparison with simulated experiments taking the instrument characteristics and well-known sample properties into account.

In the present work, we want to bring forward to development of the so-called Bragg edge transmission technique as part of the neutron imaging applications. In the past, many advances have

been achieved in neutron imaging [3]. Especially energy-resolved neutron transmission has enabled the possibility to investigate and visualize the effects of crystallographic structures and their properties. The basic principle of such investigations is the analysis of patterns occurring in the transmission spectrum – the Bragg edges. According to Bragg's law, these sudden intensity changes appear due to coherent elastic scattering of neutrons with wavelength λ at selected *hkl* lattice planes with interplanar distance *d*.

$$n\lambda = 2d_{hkl} \sin\theta \tag{1}$$

The scattering angle is denoted with θ and *n* is the order of the reflection, which accounts for the fact that also higher orders of the wavelength might be reflected under the conditions of Bragg's law. Applying the transmission geometry, the Bragg edge phenomenon becomes visible when $\lambda = 2d$, i.e. $\theta = 90°$. For wavelengths longer than this position no Bragg scattering will be possible for the selected lattice plane. The reason for the sudden intensity increase is that the fraction of neutrons to be scattered by this lattice plane disappears at this point – more neutrons can contribute to the transmitted intensity. As a result, the step-like Bragg edges occur in the transmission spectrum. A simulation of this effect and the prediction of Bragg edges are of considerable benefit for any beamline concerned with such measurements and for anybody who plans or performs such experiments. Thus, appropriate measurement positions will be known beforehand. Moreover, the performance of future imaging instruments [4] using the Bragg edge mode could be estimated, if a calculation of this effect is available.

Since, coherent elastic scattering is responsible for the Bragg transmission edges it seems obvious that crystal structure information can be derived from such measurements. Here, we refer to the analysis of crystallographic preferred orientations, known as texture [5], and lattice strains, induced by residual stresses for example [6]. Therefore, different samples featuring these properties have been investigated on instruments utilizing different methods to enable wavelength-dispersive neutron transmission experiments. A simulation of these approaches including the sample features is demonstrated in this paper, which allows conclusions to be drawn about the quantitative analysis of the crystallographic properties using the Bragg edge transmission method.

2. Neutron energy selection and detection

In order to realize Bragg edge experiments, different approaches exist. In principle, wavelength-sensitive neutron transmission is performed either by selecting a single wavelength prior to the sample – scanning through a series of wavelengths and measuring the transmission signal for each step – or by analyzing the complete spectrum of a transmitted beam at the detector position, for example in terms of the neutron time-of-flight (ToF) method. Both methods have been utilized within this work, namely on the CONRAD tomography machine and the (very) small angle neutron scattering instrument VSANS, both at the BER II continuous source of the Helmholtz Centre Berlin (HZB), and the ENGIN-X diffractometer at the ISIS pulse spallation source, UK.

2.1. CONRAD tomography instrument

The CONRAD instrument is dedicated to radiography and tomography experiments using a spectrum of cold neutrons with wavelengths between 2 Å and 12 Å [7]. The instrument setup includes an option to select a monochromatic incident beam (see figure 1). Therefore, a double-monochromator device [8] is installed to scan through individual wavelengths by rotating and shifting two highly-orientated pyrolytic graphite (HOPG) single crystals according to the Bragg equation (1). With this setup a wavelength resolution of $\Delta\lambda/\lambda \approx 3\%$ is achieved. The specimen is mounted on a translation and rotation table 5 m away from the monochromator position, followed by the detector stage. A ZnS/^{6}Li scintillator screen converts the neutron intensity to visible light captured by a CCD camera, which is reflected upwards for shielding reasons.

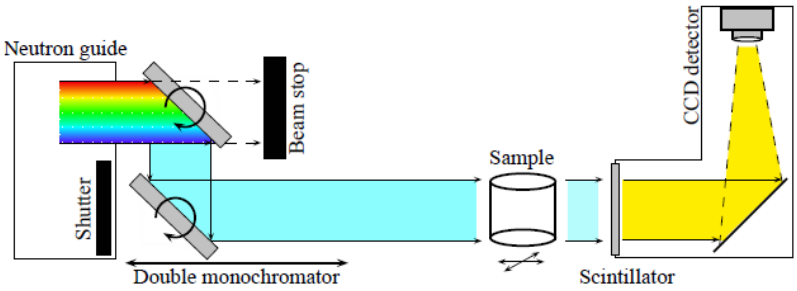

Figure 1. Basic principle of the CONRAD tomography machine using a double-monochromator device: The monochromator crystals are aligned according to Bragg's equation (1) to select single wavelength from the incident cold neutron spectrum.

2.2. VSANS instrument

The VSANS instrument is located at the neutron guide NL4C of the BER II providing a cold neutron spectrum with a lower limit of around 3.5 Å. The principle setup is visualized in figure 2, which shows the workflow of the chopper system along the neutron guide. Initially, a supermirror coated multichannel bender extracts neutrons to the neutron guide which has a window of 4 × 4 cm^2 at the beginning and 8 × 8 cm^2 at the end. In between, four chopper discs create a pulsed beam from the incident continuous beam. After that, a collimation chamber, consisting of variable neutron guide sections, can be utilized to measure with different divergence settings. The geometry and the wavelength selection of the new VSANS instrument were used to measure neutron transmission in the Bragg edge region, such that the original sample position was modified. Within a proof-of-principle study [9], the position at the end of the detection chamber was used for the sample position and the detection system. The latter was a CCD camera to take radiographic images triggered with a MCP amplifier to measure the transmitted neutron intensity versus the neutron ToF. The total distance of the detector system was L = 31.85 m away from the master chopper. In order to resolve the neutron wavelength λ, the measured ToF signal t is converted using the de Broglie relation:

$$\lambda = \frac{ht}{mL} \tag{2}$$

Where h is Planck's constant and m is the neutron mass. The original sample position applied for small angle scattering experiments is located 20 m downstream from the first (master) chopper – the place between both chambers. Here, a pinhole with a diameter of 3 cm has been used for the imaging experiment presented in this work.

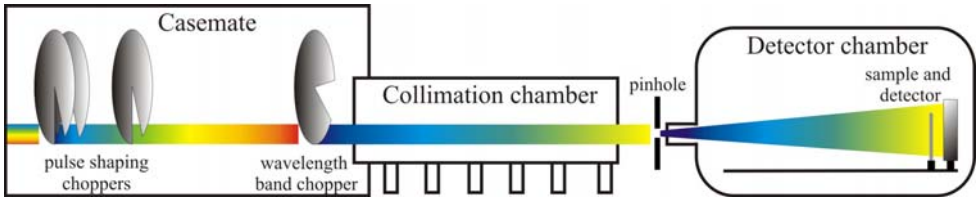

Figure 2. Schematic drawing of the VSANS instrument: The continuous neutron signal is transformed into a pulsed beam using rotating disc choppers. For the experiment presented in this paper, the sample and detector stage was placed at the end of the detector chamber.

2.3. ENGIN-X diffractometer

ENGIN-X is a time-of-flight diffractometer designed to study residual stresses of engineering materials with neutrons [10]. Viewing a 100K liquid methane moderator, the instrument provides a

spectrum of approx. 0.5 Å to 6 Å with a high-flux range over 1 Å to 3 Å [11] at a moderator-sample distance of L = 50 m. Therefore, two detector banks located 1.5 m away from the sample table and ±90° from the incident beam direction are installed to measure the ToF signal. In addition to the diffraction mode, the instrument is able to measure the neutron intensity in the transmission direction. A third detector system, consisting of a 10 × 10 array of 2 × 2 mm^2 scintillating ToF detector elements on a vertical and horizontal pitch of 0.5 mm, is placed behind the sample table to measure the neutron transmission signal. Figure 3, visualizes the instrument setup. Each detector element is connected to a Hamamatsu H6568 photo-multiplier tube via fiber optic light guides [12] and triggered with the neutron pulse frequency to count the neutron intensity against the neutron time-of-flight. Thus, transmission spectra in the Bragg edge region can be recorded.

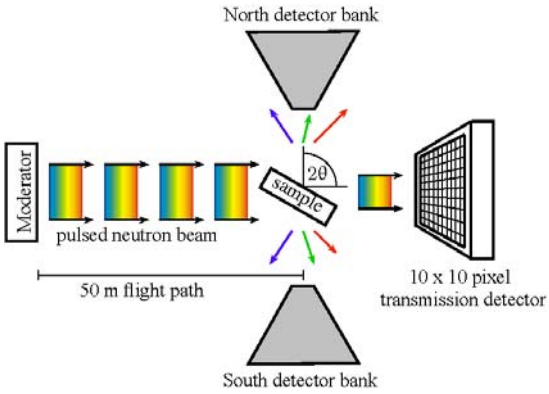

Figure 3. The ENGIN-X residual stress diffractometer at the ISIS pulsed spallation source measures the diffracted neutron intensity versus the time-of-flight. For Bragg edge measurements, the instrument is equipped with a detector array placed behind the sample.

3. Samples and reference measurements

Within this study a number of samples provided with different characteristics, namely strain and texture properties, have been investigated. All samples have also been investigated with neutron diffraction techniques in order to provide reference values from a conventional and well-established measurement method. Thus, a comparison with the Bragg edge transmission results will be possible. Further, the reference values will be used as input parameters for the developed simulations.

3.1. Residual stress samples

For the analysis of strain parameters an Al shrink-fit ring and plug cylinder has been used as a reference sample. The sample was part of the VAMAS TWA20 round-robin exercise and its strain values have been determined many times [13]. With neutron diffraction, the lattice strain was measured by means of the lattice spacing d along the sample diameter. Using the value for the unstrained lattice spacing d_0 of the same material, the strain ε is then calculated by:

$$\varepsilon = \frac{d - d_0}{d_0} \tag{3}$$

Moreover, an analytical solution to the stress and strain gradients is available due to the knowledge of its manufacturing parameters. The height and diameter of the cylinder are each 5 cm. Furthermore, a reference plug with a diameter of 2.5 cm was available to provide a specimen with the same material for measurements of the stress-free lattice parameter d_0. A photograph of the ring and plug samples and the theoretical values for the three principle strain directions (hoop, radial and axial) are shown in figure 4a and 4d respectively.

Furthermore, dieless-drawn steel rods [14] shown in figure 4b have been investigated on the E3 residual stress diffractometer at the HZB [15] to obtain the strain values along the sample diameter from the three principle directions. The sample symmetry is similar to that from the ring and plug sample, i.e. the hoop, radial and axial strains have been measured using the angular-dispersive (constant wavelength) mode on E3. The steel rods have an initial diameter of 5 mm which was drawn down to 3.5 mm. However, for a comparison with the strain data obtained with the Bragg edge method

(see section 6), we refer to the 'untreated' 5-mm-region. Here, the strain values obtained on the E3 diffractometer are plotted in figure 4e.

3.2. Texture sample

The crystallographic orientation distribution of a drawn aluminium wire sample was determined by means of pole figure measurements conducted on E3 at HZB and the STRESS-SPEC diffractometer at FRM-II [16, 17]. Therefore, an Eulerian cradle was employed to tilt and rotate the sample, such that every possible grain orientation was measured by means of the reflection intensities. A picture of the sample is shown in figure 4c, where RD indicates the rolling or reference (drawing) direction of the cylinder piece. The height of the cylinder is 8 mm and the diameter is 11.8 mm. The resulting pole figures reveal a circular symmetry around the sample axis RD which is known as fiber texture. Exemplarily, the pole figure of the (111) reflection is shown in figure 4f. The texture data is used as a reference for the comparison with the Bragg edge method.

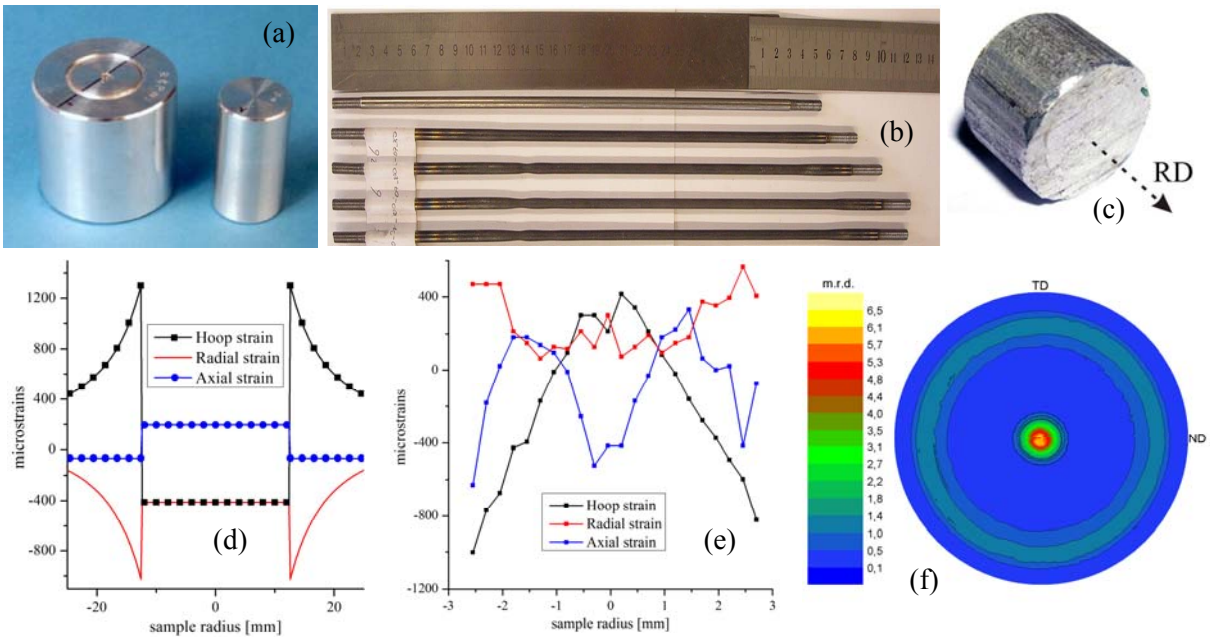

Figure 4. Investigated samples and reference data: The ring and plug Al samples (a) from the VAMAS TWA20 round-robin exercise [13] and dieless-drawn steel rods (b) [14] for residual stress investigations and a fiber-textured Al cylinder (c). The dedicated reference data is shown below: the theoretical strain values of the ring and plug (d) from the analytical solution, the strain data of the rod specimens measured on E3 (e) and a selected pole figure of the textured Al cylinder (f).

4. Development of a neutron experiment simulation

The McStas neutron ray-tracing software package [18, 19] has been utilized for the present study. McStas provides virtual neutrons propagating through an instrument emulating the conditions of a real neutron instrument. Therefore, the McStas library already includes modules that represent the individual assembly of a real instrument. These modules are ready to use and cover devices such as neutron-producing sources, guide components, slit systems, samples and detectors. Thus, each of the previously described CONRAD, VSANS and ENGIN-X machines has been mapped to a simulation taking the experimental conditions into account. Although, a few sample modules for different purposes are available, a new virtual sample simulating the Bragg edge neutron transmission effect has been developed.

4.1. Bragg edge sample module

The basic principle in McStas of a neutron propagating from the source to the end of the instrument definition (e.g. to a detector position), is to change its state parameters, i.e. its position, its flight direction and its velocity, according to the physics implemented in each of the instrument's components. In the case of the wavelength-dispersive neutron transmission method a sample module must therefore handle the neutron-matter interaction with respect to the neutron wavelength λ and the sample's crystal structure. A new sample component for McStas was created to account for these parameters and to realize Bragg edge experiment simulations.

The probability for a neutron to be transmitted is based on the computation of neutron cross sections, which describe quantitatively the interaction between neutrons and matter. The total microscopic neutron cross section σ_{total} of an isotope is the cross sectional area "presented" to an incoming neutron to interact with the material. The sum of its individual coherent, incoherent and absorption contributions (σ_{coh}, σ_{inc}, σ_{abs}) is used to determine the transmission probability *Tr*:

$$\sigma_{total}(\lambda) = \sigma_{coh}(\lambda) + \sigma_{inc}(\lambda) + \sigma_{abs}(\lambda)$$
$$Tr = \frac{I}{I_0} = \exp\left(-\sigma_{total}(\lambda)\, N\, l\right) \tag{4}$$

The transmitted intensity I is given by an exponential attenuation of the incident intensity I_0. N is the number of scattering centers per unit volume and l is the transmission path length through the sample. With λ being in the range of interatomic distances, i.e. for thermal and cold neutrons, the transmission spectrum of crystalline samples displays Bragg edges, which occur due to the discontinuities in the coherent elastic part of the neutron cross section:

$$\sigma_{coh}^{el}(\lambda) = \frac{\lambda^2}{2V_0} \sum_{d_{hkl}=0}^{2d_{hkl}<\lambda} \left|F_{hkl}\right|^2 d_{hkl} \tag{5}$$

The summation runs over all set of *hkl* lattice planes as long as d_{hkl} is smaller than half the size of the selected neutron wavelength. F_{hkl} is the structure factor and V_0 is the unit cell volume. Thus, sudden intensity changes at $\lambda = 2d_{hkl}$ in the transmission spectrum can be quantified.

The calculation of the coherent elastic scattering cross section can be applied to single atoms as well as to material compositions. However, the knowledge of the sample's crystallographic structure, its lattice parameters and the position of atoms included inside the unit cell is required. For the new sample module all parameters will be provided as input parameters to the McStas simulation. Thus, different materials and sample characteristics can be tested with the same module. The choice for a single neutron intersecting the sample volume to be transmitted is then based on the probability *Tr*, calculated by equation (4). The incoherent and absorption contributions are described elsewhere [20] and have been implemented as well.

4.2. Texture modification

Unlike powders, most engineering materials and components reveal a crystallographic preferred orientation due to the process of their manufacturing. In the case of diffraction experiments, the intensities captured with a detector vary with the number of orientated grains inside a polycrystalline sample. If the sample is textured, the probability of detecting grains via selected lattice planes differs with the sample orientation, such as shown with the pole figure in figure 4f, where the intensities, normalized to multiples of a random distribution (m.r.d.), are plotted against the sample orientation.

In order to correct for the influence of crystallographic preferred orientations, the March-Dollase model was used to apply changes to the diffraction intensities. Following the descriptions from [21], the texture model was implemented with respect to the Bragg edge transmission geometry. Hence, any correction factor will also affect the transmission spectrum. The basic principle of this model is to correct the diffraction intensities using the March-Dollase equation:

$$P_{\vec{H}}\left(\alpha_{\vec{H}}\right)=\left(r^2\cos\alpha_{\vec{H}}+\frac{1}{r}\sin^2\alpha_{\vec{H}}\right)^{-\frac{3}{2}} \tag{6}$$

where $\alpha_{\vec{H}}$ is the angle between the preferred orientation direction $\vec{H}$ and orientation axis, for example the rolling direction, and r is a variable describing the degree of the texture. Within the computation of the neutron cross sections inside the Bragg edge simulation module, the correction is applied to the calculation of the individual coherent elastic scattering cross section for each contributing lattice plane with the normal vector $\vec{h}$ and $\alpha_{\vec{h}}$ being the angle between $\vec{h}$ and the preferred orientation axis:

$$\sigma_{coh}^{el}(\lambda)=\sum_{\vec{h}}\sigma_{coh,\vec{h}}^{el}(\lambda)P_{\vec{h}}\left(\alpha_{\vec{h}}(\lambda)\right) \tag{7}$$

Basically, the procedure is to derive the correction functions $P_{\vec{h}}$ for the individual reflections $\vec{h}$ from the master correction function $P_{\vec{H}}$ [21]. Thus, a simulation of texture influences parameterized by only two values, $\vec{H}$ and r, is realized using McStas and the developed Bragg edge module.

4.3. Strain implementation

A second modified version of the Bragg edge sample module was created to include local variations of lattice spacings, i.e. strain. The basic principle of the calculation implemented in the sample module is shown in figure 5 and is explained based on the example of the ring and plug cylinder sample.

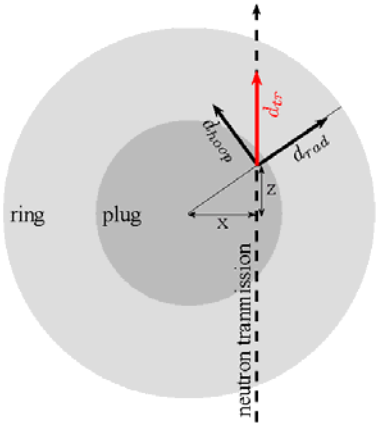

Figure 5. The calculation of the effective lattice spacing d_{tr} considers the neutron position within the sample as well as the flight direction. The lattice spacing values in the principle strain directions are chosen according to the position on sample radius. In this figure, the calculation is simplified to the *xz*-plane (hoop and radial strain).

In order to ensure a realistic calculation, the computation of the lattice spacing in the transmission direction not only depends on the spatial position inside the sample but also on the neutron flight direction. Hence, the three strain components (radial, hoop, axial) are utilized to calculate the effective d-value in the neutron flight direction:

$$\begin{aligned} d_{xz} &= \left(d_{hoop}-d_{rad}\right)\sin^2\psi_1+d_{rad} \\ d_{tr} &= \left(d_{xz}-d_{axial}\right)\sin^2\psi_2+d_{axial} \end{aligned} \tag{8}$$

In a first instance, the lattice spacing d_{xz} in the *xz*-plane (see figure 5) is determined based on the neutron flight direction in that plane, where ψ_1 is the angle between d_{xz} and the radial component d_{rad}. In the second step the axial strain is applied to account for any neutron direction outside the *xz*-plane. Hence, ψ_2 is the angle between the neutron flight direction and the y-axis (height) of the sample cylinder. For both steps, the $sin^2\psi$ approach is utilized, which assumes that the lattice spacing is linear with the square of sine of the angle between two principle directions [22]. Thus, the calculation of the effective d-value d_{tr} along the neutron transmission path also considers any degree of beam divergence and therefore accounts for the influences of the instrument parameters. Since every neutron is considered individually during the simulation, the computation of the appropriate d-value is performed

for every neutron passing through the sample. The decision whether a virtual neutron is transmitted depends again on the probability calculated with equation (4) – but this time using the value of d_{tr} computed for each individual neutron. As a result the position of a Bragg edge in the transmission spectrum is affected by the lattice strain in the sample. As the experiments follow a radiographic approach, the detected signal is a convolution of all effective lattice spacings along the transmission path through the sample. Hence, the strain values evaluated from such measurements will be referred to as the "projected" strain.

5. Experiments and simulations

Utilizing the presented instruments, different methods have been applied to measure Bragg edges and the properties of the investigated samples.

On CONRAD, an iterative alignment of the double-monochromator device has been conducted to perform a wavelength scan from 3 Å to 5 Å in steps of 0.01 Å and 0.02 Å for the ring and plug residual stress specimen and the textured Al cylinder respectively. The radiographic images taken by the CCD camera have been normalized by flatfield measurements to correct for the incident intensity variation and the inhomogeneous screen illumination. The images in figure 6 show the corrected radiographs for selected wavelength positions for both experiments. The resulting grey values have been used to analyze the transmission spectrum. Thus, the Bragg edge positions could be identified. In order to improve the statistics, the evaluated regions along the diameter of the ring and plug sample have been selected with regions of interest of 4.5 × 9 mm^2 each, to determine a single grey value for each wavelength step. These regions are indicated in figure 6a. For the textured sample (figure 6b), the region of the circular base area was analysed.

The same samples have been investigated on ENGIN-X measuring the ToF signal with the transmission detectors, i.e. the complete transmission spectrum from 2 Å to 5 Å has been captured at once. The samples were aligned such that the middle of the array detector was faced with the sample center. Because of the limited detector size and the field of view, the ring and plug sample was driven sideways from -25 mm to +25 mm in 5 mm steps to scan through the sample diameter with the center of the detector array. For each step, transmission spectra have been recorded by each of the detector elements. Initially, the 6th detector column was aligned to the sample center (radius r = 0 mm), such that the 7th column faced the position at r = 2.5 mm.

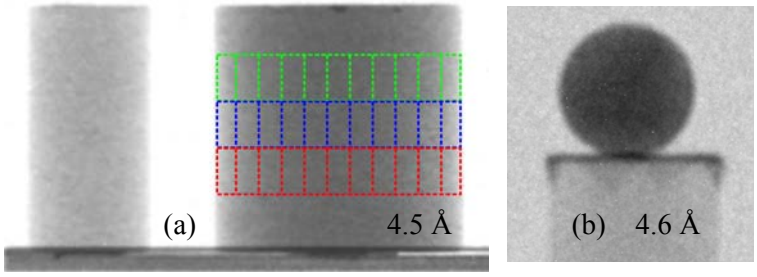

Figure 6. A normalised radiograph of the reference plug (left) and the ring and plug sample (right) are shown in (a). The coloured regions mark the areas along the sample diameter that have been evaluated. In (b) the texture cylinder, placed on a sample table, is shown.

The parameters used to run the presented experiments have been transferred to the developed Bragg edge simulation using McStas, i.e. the program has been executed using the same arrangements as the real experiment. In particular, this refers to the wavelength scans and the additional flatfield measurements performed with CONRAD. Although, it is possible with McStas to record the neutron state parameters (including the neutron wavelength) at any time during the simulation and thus a distinction between individual wavelengths in the transmission spectrum would be enabled, the study was focused on the influence of the double-monochromator. Hence, the device was included in the simulation and aligned stepwise such that the wavelength scans mentioned above could be emulated. The ring and plug sample has been included in terms of the developed Bragg edge sample module. The residual stress properties have been inherited from the theoretical strain values from figure 4d such that a calculation of the effective lattice spacings along the neutron transmission direction has been enabled as described in section 4.3.

The dieless-drawn steel rods have been measured on the VSANS machine. Therefore, the incident neutron beam has been transformed into a pulsed beam such that the neutron ToF signal could be triggered with the CCD camera in order to map the transmitted intensity to individual wavelengths. Details of the experimental setup and the chopper settings to realize a constant wavelength resolution of about $\Delta\lambda/\lambda$ = 1.5 % for a wavelength band from 3 Å to approximately 5 Å have already been reported in [9]. A simulation of the complete VSANS machine is currently under development. However, the experimental parameters have been applied to the Bragg edge simulation using the strain parameters shown in figure 4e for the dieless-drawn steel specimens.

6. Results and Comparison

6.1. Texture Al cylinder

In figure 7, the measured and simulated transmission spectra of the textured cylinder sample are shown. Using the incident and transmitted neutron intensities, the attenuation coefficient was used to compare the results with the theoretical texture-free Bragg edges. It is apparent, that the resulting spectra show large deviations due to the influence of crystallographic preferred orientations. Especially the (111) Bragg edge at 4.6 Å reveals a large increase of the macroscopic cross section which coincides with the intensity in the center (RD) of the pole figure shown in 4f. Furthermore, a difference between the CONRAD and ENGIN-X results can be observed. In particular, the height of the Bragg edge varies by a factor of around 2.5, which is a result of the wavelength-selection with the double-monochromator. The wavelength resolution of 3% smears the evaluated attenuation coefficient due to wavelengths before and after the selected position.

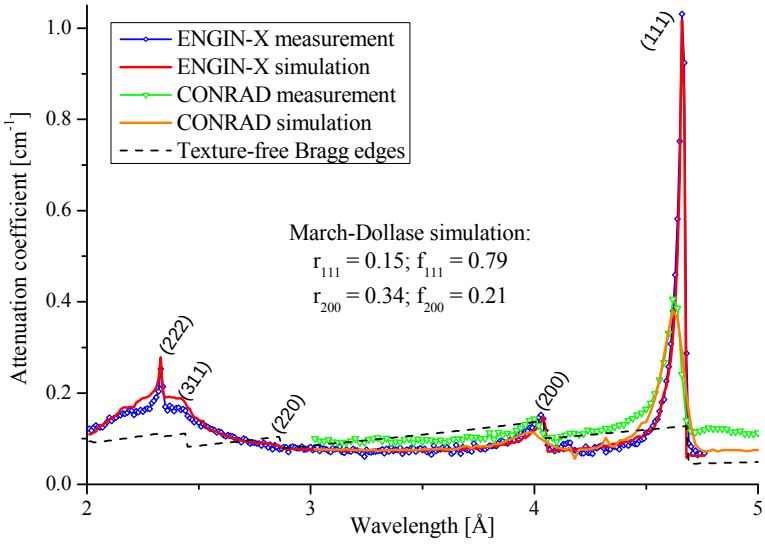

Figure 7. Comparison of the transmission spectra of the textured Al sample measured and simulated with the CONRAD and ENGIN-X instruments. Compared to the texture-free curve (dashed) the Bragg edges captured in RD show large deviations due to preferred crystallographic orientations.

Nevertheless, the simulations, executed with the March-Dollase modification, agree with the individual experiments. Therefore, the same March-Dollase parameters have been applied for both, the CONRAD and ENGIN-X simulations. As shown in the figure, two preferred orientation directions (111 and 200) were used for the simulation. Here a further parameter *f* was established to account for the fraction of grains exhibiting one of the given directions. Thus, a good agreement with the ENGIN-X data could be achieved. Only a small misfit in the region of the (311) and (222) Bragg edge can be found. The CONRAD results also show the same trend. The difference between simulation and experiment, appearing like a vertical shift, occurs due to the uncertainties of the monochromator description. For the simulation, a single value has been used to describe the mosaic spread of the two applied single crystals. Moreover, the strength of higher-order reflections from the monochromator contributing to the measured intensity is unknown, which could lead to the deviations shown.

6.2. Ring and plug

The strain values of the ring and plug sample have been compared similarly. Therefore, the Bragg edge positions of the measured and simulated transmission spectra from ENGIN-X have been fitted to a function proposed in [23], which accounts for the asymmetric and symmetric instrument broadenings affecting the Bragg edge. For the CONRAD results, the same function with a modified kernel has been used to fit the data. Here, a single parameter σ was used to describe the instrumental broadening.

$$Tr(\lambda) = \exp(-n\omega\sigma_0)\left\{\exp(-n\omega\sigma_{hkl}) + (1-\exp(-n\omega\sigma_{hkl}))\frac{1}{2}erfc\left(-\frac{\lambda-\lambda_0}{\sqrt{2}\sigma}\right)\right\} \quad (9)$$

The atomic density n, the sample thickness ω and the total neutron cross sections σ_{hkl} and σ_0 at the short and long wavelength side of the selected *hkl* edge can be defined before the fitting. The fit result is the Bragg edge position at λ_0. The resulting projected strains, calculated with equation (3), are shown in figure 8.

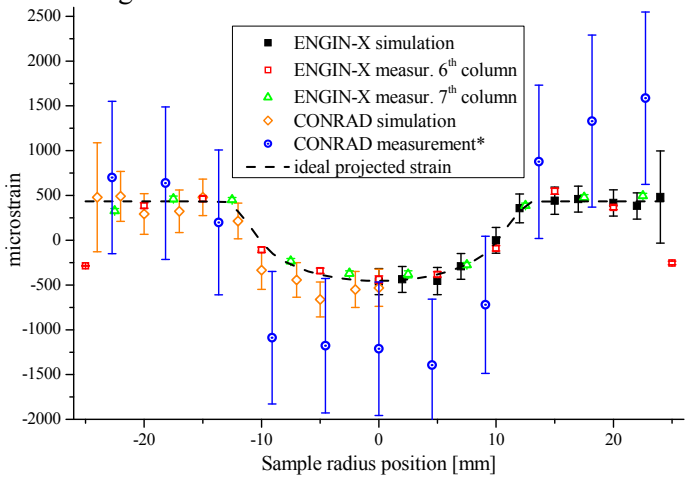

Figure 8. The projected strains in the transmission direction evaluated from measurements and simulations of the CONRAD and ENGIN-X instruments are compared with the ideal strain curve (dashed line). The asterisk at the CONRAD measurement curve indicates that the error bars have been scaled down by a factor of 5 for reasons of clarity.

The plotted results follow the same trend of the ideal projected strain (dashed curve) that was obtained from the calculations presented in section 4.3. The best fit to that reference results from the ENGIN-X experiment and simulation data. This is also true for both evaluated detector columns (6^{th} and 7^{th}. The only mismatch occurs at the two sample edge positions at ±25 mm, because for these positions the 2 × 2 mm^2 detector element is covered by only half of the sample area. The rest already faces neutrons outside the sample volume, which affects the fitting of Bragg edge position systematically. Moreover, it is visible that the error bars become larger with an increasing radius position due to the fact that the sample gets thinner which downgrades the statistics.

The strains obtained on CONRAD exhibit the largest deviation from the reference. The standard deviation of the data set about the ideal projected strain suggests a random error of about 750 microstrain (the size of the error bars depicted here). However, the actual fits from the fitting routine used returned much larger uncertainties (an average of about 2500 microstrain if one does not include the uncertainty of the reference specimen and 4000 microstrain if one does include the reference uncertainty). These fitting uncertainties are clearly unrealistic. The comparison of the data sets depicted above presents the opportunity to evaluate the approximate actual random uncertainty. Nevertheless, the simulation of the CONRAD experiment reveals an acceptable agreement with the dashed curve. Consequently, for the case of the strain and stress analysis the description of the simulated CONRAD instrument is not sufficiently accurate. The above mentioned uncertainties of the monochromator parameterization and the estimated wavelength resolution manifest the difficulties of Bragg edge position evaluations from CONRAD experiments.

6.3. Dieless-drawn steel rods

The untreated region of the dieless-drawn steel rods has been investigated in this study. The observed strain values measured with conventional neutron diffraction have been applied to the developed

Bragg edge simulation to obtain the theoretical projected strain for these samples. Thus, the transmission measurements on VSANS could be validated, although a model of the instrument is not yet available. In figure 9, the ideal projected strain (dashed curve) is compared with the measured curves evaluated based on a 5 × 5 binning of the captured radiographic images [9].

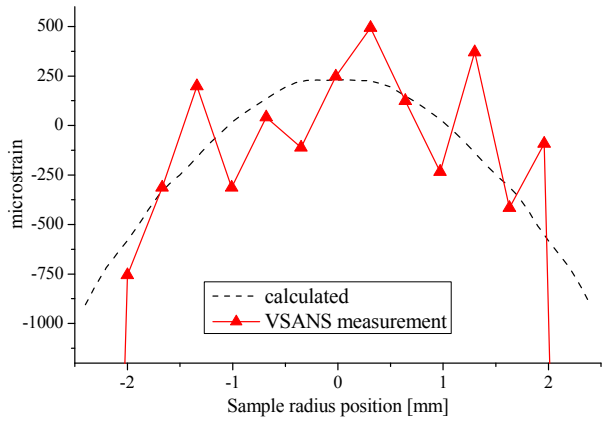

Figure 9. Comparison of the measured and calculated projected strain along the sample diameter of a dieless-drawn steel rod.

The diagram shows that the evaluated strain along the sample diameter follows the expected trend of the calculated projected strain. The variations occur due to the limited neutron statistics and the thin samples, in particular at the sample edge.

7. Conclusion

We have created new program routines for the calculation of neutron cross sections. These routines have been used with the McStas simulation environment to represent a sample module that is able to perform realistic Bragg edge transmission simulations. The presented work has shown, that the simulation is capable to emulate different materials based on their crystallographic description. Furthermore, the McStas module was modified for two cases to simulate texture and strain properties. The former was achieved by the application of the March-Dollase model, which enables to adjust the Bragg edge spectrum according preferred crystallographic orientations based on two parameters. The latter has been realized using the strain values measured with conventional diffraction methods. The calculation of the effective strain in the transmission direction was implemented and applied to determine the measureable projected strain.

Regarding the analysis of strain properties applied the Bragg edge method, the ENGIN-X instrument showed the best results. The main beneficial aspect here is the wavelength resolution of the instrument, which was given in [24] in terms of the lattice spacing precision of $\Delta d/d = 10^{-4}$. Hence, the ToF diffractometer suggests the reliability for further experiments of this kind. In contrast, the wavelength-selective option on CONRAD could not provide such results. However, the simulation showed, that the lower resolution could also deliver comparable results. As a consequence, the parameterization of the double-monochromator for the simulation requires further investigations. In between, the 1.5% wavelength resolution of the VSANS setup has proven the feasibility of the strain measurements. However, the agreement to the calculated reference data may be improved.

From the analysis of the textured Al sample cylinder on the CONRAD and ENGIN-X instruments several conclusions can be drawn. Both the ENGIN-X measurement and simulation showed very good agreement and the strength of the texture coincides with the reference pole figure measurements obtained with neutron diffraction. The CONRAD results show a considerably smaller degree of texture due to wavelength spread of the monochromator mosaicity. However, using the simulation and applying the same March-Dollase parameters from the ENGIN-X, the same texture influence on the Bragg edge spectrum was reproduced with McStas. Nevertheless, more powerful texture models may be needed if more complex samples shall be investigated.

In summary, a Monte Carlo application was developed to validate measured strain and texture data with Bragg edge neutron transmission and to provide test cases for further investigation regarding instrument developments.

Acknowledgements
We would like to thank Javier Santisteban, Jon James, Brian Abbey, Daniel Clemens, Christian Randau and Michael Hofmann for their support with the instruments and the helpful discussions on the experimental methods. We thank Peter Tiernan for permission to reprint figure 4b.

References

[1] Šaroun J, Pirling T and Rogge R B 2002 *Appl. Phys. A* **74** s1489-s91
[2] Santisteban J R, Daymond M R, James J A and Edwards L 2006 *J. Appl. Cryst.* **39** 812-25
[3] Strobl M, Manke I, Kardjilov N, Hilger A, Dawson M and Banhart J 2009 *J. Phys. D: Appl. Phys.* **42** 243001
[4] Kockelmann W, Zhang S Y, James J A, Burca G, Paradowska A and Chapon L 2009 IMAT: An Imaging and Engineering Facility for ISIS TS-II *Proc. NEUWAVE2 (Abingdon, UK, July 12-15, 2009)*
[5] Bunge H-J 1993 *Texture Analysis in Materials Science: Mathematical Methods* (Göttingen: Cuvillier Verlag)
[6] Hauk V 1997 *Structural and Residual Stress Analysis by Nondestructive Methods: Evaluation - Application - Assessment* (Amsterdam: Elsevier Sience)
[7] Hilger A, Kardjilov N, Strobl M, Treimer W and Banhart J 2006 *Physica B* **385** 1213-5
[8] Treimer W, Strobl M, Kardjilov N, Hilger A and Manke I 2006 *Appl. Phys. Lett.* **89** 203504
[9] Strobl M *et al.* 2010 *Nucl. Instrum. Methods Phys. Res., Sect. A* in press
[10] Dann J A, Daymond M R, James J A, Santisteban J R and Edwards L 2003 ENGIN-X: A New Diffractometer Optimised for Stress Measurement *Proc. ICANS XVI (Düsseldorf-Neuss, Germany, May 12 - 15, 2003)* eds G Mank and H Conrad pp 231-8
[11] Kockelmann W, Frei G, Lehmann E H, Vontobel P and Santisteban J R 2007 *Nucl. Instrum. Methods Phys. Res., Sect. A* **578** 421-34
[12] Santisteban J R, Steuwer A, Edwards L, Withers P J and Daymond M R 2003 Phase analysis and imaging by TOF neutron transmission *Proc. ICANS XVI (Düsseldorf-Neuss, Germany, May 12 - 15, 2003)* eds G Mank and H Conrad pp 239-46
[13] Webster G A 2000 *Neutron Diffraction Measurements of Residual Stress in a Shrink-fit Ring and Plug* (Teddington, UK: VAMAS Report No. 38, National Physics Laboratory)
[14] Carolan R and Tiernan P 2009 *J. Mater. Process. Technol.* **209** 3335-42
[15] Wimpory R C, Mikula P, Šaroun J, Poeste T, Li J, Hofmann M and Schneider R 2008 *Neutron News* **19** 16-9
[16] Hofmann M, Rebelo-Kornmeier J, Garbe U, Wimpory R C, Repper J, Seidl G A, Brokmeier H-G and Schneider R 2007 *Neutron News* **18** 27-30
[17] Brokmeier H-G, Gan W M, Randau C, Völler M, Rebelo-Kornmeier J and Hofmann M 2011 *Nucl. Instrum. Methods Phys. Res., Sect. A* **642** (1) 87-92
[18] Lefmann K and Nielsen K 1999 *Neutron News* **10** 20-3
[19] Willendrup P K a r 2004 *Physica B* **350** E735-E7
[20] Granada J R 1984 *Z. Naturforsch. A* **39** 1160-7
[21] Vogel S C 2000 *A Rietveld-Approach for the Analysis of Neutron Time-Of-Flight Transmission Data* PhD thesis Christian-Albrecht-Univ. Kiel
[22] Fitzpatrick M E and Lodini A 2003 *Analysis of Residual Stress by Diffraction using Neutron and Synchrotron Radiation* (London: Taylor & Francis)
[23] Santisteban J R, Edwards L, Steuwer A and Withers P J 2001 *J. Appl. Cryst.* **34** 289-97
[24] Steuwer A, Santisteban J R, Withers P J, Edwards L and Fitzpatrick M E 2003 *J. Appl. Cryst.* **36** 1159-68